Arch. Metall. Mater. **66** (2021), 1, 15-23

DOI: 10.24425/amm.2021.134753

M. MATEJKA[1*], D. BOLIBRUCHOVÁ[1], M. CHALUPOVÁ[2]

STUDY OF THE PROPERTIES OF THE AlSi9Cu3 ALLOY DEPENDING ON THE RATIO OF RETURNABLE MATERIAL IN THE BATCH

Recycling of aluminium returnable material through its reuse is now an essential component of the production of aluminium alloy castings. The main goal is to find a suitable ratio of the primary alloy and the returnable material in the batch, thus determining the right compromise between the price and the quality of the casting. Experimental alloys were evaluated by thermal analysis, combination of structural analytical techniques and selected mechanical properties. The alloys were also subjected to tearing susceptibility testing. The increase in the returnable material amount resulted in changes in the alloy properties at the first increase in volume to 20%. After exceeding the balanced ratio (50:50), there was considerable degradation of the microstructure, failure to achieve the minimum values of some mechanical properties required by the standard, and the alloy showed increased susceptibility to tearing.

Keywords: Al-Si-Cu cast alloys, natural and artificial ageing, metallography, mechanical properties, hot tearing

1. Introduction

Nowadays, almost 100% of the waste from the production of aluminum products is recycled. A major part of the use (approximately 70%) of recycled aluminum is in the production of aluminum alloys cast mainly for the automotive industry components [1]. Secondary aluminum metallurgy, as well as many other recycling processes, is an important issue from an economic and environmental perspective. For this reason the foundries today use in batches an increasing amount of returnable material, which may account for several tens of percent of the total batch. However, the recycling process through remelting may cause some change in the melt quality. In particular, there can be changes in the chemical composition [2].

In the case of secondary alloys, the intermetallic phases can be analyzed on the cooling curve that are rich in another element, which made its way to the alloy in the form of impurities, for example. The most common impurity element occurring in aluminum alloys is iron [3]. The negative effect of iron begins to manifest at its low amount levels and is accompanied by a decrease in tensile strength and ductility. When the critical iron content is exceeded, these characteristics deteriorate significantly. Increasing the silicon content in the alloy increases the permissible amount of iron before the beginning of the β-phase formation, when the Al-Si eutectic begins to form [4]. According to Taylor, the negative effect of iron on ductility is caused by an increase in the number and size of iron-based intermetallic phases that are directly involved in the fracture mechanism. An increase in the iron content results in an increase in porosity with a consequent decrease in ductility. Critical Fe content in wt. % can also be calculated from the equation [5]:

$$Fe_{krit} \approx 0.075 \times (\%\ Si) - 0.05 \quad (1)$$

The presence of copper as an additive element allows the application of heat treatment by precipitation hardening. The process of natural aging is slow and spontaneous. The final properties are achieved after 100 to 150 hours, therefore mechanical tests and machining are prescribed only after this time due to the longer hardening time [6]. The precipitation process begins with the diffusion of the additive element into the microscopic regions richer in the given element and that is where nucleation of a new phase occurs. The growth of these nuclei results in coherent precipitates known as the Guinier-Preston zones (GPZ). Coherence indicates that these regions are part of the solid solution crystalline lattice, thereby causing lattice deformation and induction of internal stresses in it. The induced stresses are the cause of increasing strength and hardness of the alloy [7].

[1] UNIVERSITY OF ŽILINA, FACULTY OF MECHANICAL ENGINEERING, DEPARTMENT OF TECHNOLOGICAL ENGINEERING, UNIVERZITNÁ 8215/1, 010 26 ŽILINA, SLOVAKIA
[2] UNIVERSITY OF ŽILINA, FACULTY OF MECHANICAL ENGINEERING, DEPARTMENT OF MATERIALS ENGINEERING, UNIVERZITNÁ 8215/1, 010 26 ŽILINA, SLOVAKIA

* Corresponding author: marek.matejka@fstroj.uniza.sk

It is known from the literature specializing in aluminum alloys that several factors influence tearing formation. The main factors probably include the effect of chemical composition, casting temperature, mold temperature and, last but not least, the design of the mold. The chemical composition has a profound effect on the resulting alloy susceptibility to tearing formation, whether it be individual elements or the solidification interval length, which is directly related to the chemical composition. In general, the longer the solidification interval, the higher the susceptibility of the alloy to tearing formation [8].

2. Experimental materials and methods

Hypoeutectic AlSi9Cu3 alloy (EN AC – 46 000) was chosen to evaluate the effect of the increasing ratio of returnable material in the batch. The alloy is characterized by medium mechanical properties, good strength at elevated temperatures, and good workability. A dominant part of its usage are castings for the automotive industry that are cast mainly by pressure casting: cylinder heads and engine blocks, crankshaft cabinets, and other components [9]. Two types of AlSi9Cu3 alloys were used for the experiments. The primary AlSi9Cu3 alloy from the manufacturer and the AlSi9Cu3 alloy prepared by remelting the foundry returnable material (gating and riser systems) into ingots. The chemical composition of the primary alloy according to the standard (EN 1706), that of the primary alloy (from the manufacturer) and that of the alloy prepared by remelting the foundry returnable material is given in Table 1.

Five alloys were sequentially cast in the next part of the experiment. These alloys were designated 20 – 80; 50 – 50; 70 – 30; 80 – 20; and 90 – 10, wherein the first figure denotes the percentage of returnable material and the second figure denotes the primary alloy percentage in the batch. Melting of each alloy was carried out in an electric resistance furnace with a T15 type regulator in a graphite crucible that had been treated with a protective coating. Casting was carried out at a temperature of 750 ± 5°C. Samples were cast from each melt to test mechanical properties (10 samples) and structure analysis under the same conditions. Samples were cast into a metal mold at a temperature of 150 ± 5°C. The alloys were not refined, inoculated or modified in any way in the process, and only the oxide membranes were mechanically removed before casting. Chemical deposition of newly formed alloys is given in Table 2.

The samples for metallographic observations were prepared by standard metallographic procedures (wet ground, polished with diamond pastes, finally polished with commercial fine silica slurry) from selected tensile specimens (after testing). The microstructure of experimental material was studied using optical microscope Neophot 32 and SEM observation with EDX analysis using scanning electron microscope VEGA LMU II linked to the energy dispersive X-ray spectroscopy. Samples were etched by standard reagent (0.5 % HF). Some samples were also deep-etched for 30 s in HCl solution in order to reveal the three-dimensional morphology of the eutectic silicon and intermetallic phases. Each sample was subjected to measuring the length of the Al_5FeSi iron phase at 500x magnification. The process of crystallization of alloys with different ratio of returnable material in the batch was evaluated by thermal analysis. A K-type thermocouple (NiCr-Ni) placed in the middle of a cylindrical metal mold was used during the measurement. The values were recorded in LabView 2 Hz software. From the measured values, cooling curves were generated and their first derivatives and temperatures for the crystallization of the individual structural components of the alloy were determined.

The tensile test was performed in accordance with the STN EN ISO 6892-1 standard on testing machine WDW 20 with a maximum load of 20 kN and a constant cross-head feed rate of 2 mm/min. The Brinell hardness test was performed according to STN EN ISO 6506-1 on testing machine INNOVATEST NEXUS 3002XLM-INV1 with a load of 125kp (1226 N), 5 mm diameter ball and a dwell time of 15 s. The Brinell hardness value at each state was obtained as the average of at least six measurements. The microhardness of the structural components was evaluated using a Hanemann Mod 32 device at a load of 10p. The resulting value represents the average value of 20 measurements.

TABLE 1

Chemical composition of AlSi9Cu3 by standard, primary AlSi9Cu3 (from the manufacturer) and returnable material of AlSi9Cu3 (wt. %)

Elements	Si	Fe	Cu	Mn	Mg	Ni	Zn	Ti	Cr
AlSi9Cu3 (EN 1706)	8.0 – 11.0	0.6 – 1.1	2.0 – 4.0	0.55	0.15 – 0.55	0.55	1.20	0.20	0.15
Primary AlSi9Cu3	9.563	1.081	2.206	0.184	0.426	0.092	1.160	0.038	0.027
Returnable AlSi9Cu3	9.294	1.674	2.074	0.184	0.348	0.129	1.016	0.034	0.113

TABLE 2

Chemical composition of experimental alloys AlSi9Cu3 alloy (wt. %)

Elements	Si	Fe	Cu	Mn	Mg	Ni	Zn	Ti	Cr
20 – 80	9.507	1.294	2.197	0.231	0.391	0.122	1.044	0.035	0.049
50 – 50	9.418	1.419	2.173	0.223	0.361	0.134	1.041	0.033	0.072
70 – 30	9.245	1.569	2.02	0.209	0.344	0.108	0.961	0.031	0.112
80 – 20	9.415	1.617	2.08	0.206	0.358	0.156	1.07	0.032	0.101
90 – 10	9.291	1.643	2.143	0.199	0.357	0.127	1.046	0.032	0.106

Structural analysis of alloys and mechanical characteristics were performed on samples after natural aging (160 hours at 23°C) and on samples after heat treatment (T5 – artificial aging at 200 ± 5°C for 4 hours and cooling in water).

3. Results of experimental work

Evaluation of microstructure and thermal analysis after natural ageing

Microstructure of an alloy with 80% ration of the primary alloy (20 – 80) consists of an α-phase matrix, eutectic silicon, and iron-based intermetallic phases evenly distributed in the aluminum matrix (Fig. 1a). Grains of eutectic silicon are excluded in the so-called. unmodified shape as hexagonal plate-like crystals with non-oriented distribution (also known as unmodified eutectic in literature) with the TPRE (twin plane re-entrant edge) growth mechanism [10]. Iron-based intermetallic phase precipitates in the interdendritic and intergranular regions as platelets (appearing as needles / acicular formations in the metallographic microscope). With a balanced ratio of primary alloy and returnable material in the batch (50 – 50), the microstructure did not change significantly, only a slight increase in the lengths of the iron phase acicular formations can be observed (Fig. 1b). For alloys consisting of a larger ratio of returnable material (alloys 70 – 30, 80 – 20 and 90 – 10), the microstructure is characterized by a large number of long and thin acicular formations of iron-rich phases (Fig. 1c). An increase in the ratio of returnable material resulted in local coarsening of the eutectic silicon grains, which is noticeable at the ground plane.

Increasing the ratio of returnable material did not manifest any significant effect on the individual crystallization temperatures of the structural components. An exception is iron-based intermetallic phases. The gradual increase in the ratio of returnable material in the batch caused a linear increase in wt. % Fe in the alloys and thus a gradual increase in nucleation temperatures of these phases. The nucleation temperatures of the iron phases were at the level of T_{AlSiFe} = 574°C for the alloy with the lowest (20 – 80) ratio of returnable materials. For the alloy with a 50 – 50 balanced ratio, the temperature T_{AlSiFe} = 577°C, and for the alloy with the highest (90 – 10) ratio of returnable material the temperature T_{AlSiFe} = 584°C. Table 3 shows characteristic phase conversion temperatures for all structural components.

TABLE 3

Temperature of characteristic reaction of experimentally alloys AlSi9Cu3

Alloy	T_{Liq} [°C]	T_{AlFeSi} [°C]	T_{AlSi} [°C]	T_{AlSiCu} [°C]	T_{Sol} [°C]
20 – 80	630	574	571	542	474
50 – 50	631	577	569	541	477
70 – 30	633	579	572	542	476
80 – 20	628	581	569	545	473
90 – 10	632	584	570	543	476

Gradually increasing wt. % of Fe resulted in exceeding thr F_{krit} value in all alloys. The F_{krit} (1) value indicates that the iron-rich phases will be excluded before the eutectic silicon phases [6]. The iron intermetallic phases that are formed prior to the crystallization of the AlSi eutectic tend to form phases of much larger dimensions than those formed after the eutectic solidifies. A detailed thermal analysis of the iron phase nucleation region (Fig. 2b) confirms that the iron-rich phases were preferably excluded before the AlSi eutectic. It can also be seen from the detail that with a gradual increase in wt. % Fe the latent heat released by the crystalline conversion of these phases also increases, which may be directly related to the increase in the average lengths of the iron phases. The expected growth with a gradual increase in the ratio of returnable material was confirmed by measuring the average acicular lengths of β – Al_5FeSi phases whose presence was confirmed by line analysis (Fig. 2a). The average acicular length for the 20 – 80 alloy was 33.4 µm, and 38.6 µm for the alloy with the balanced ratio (50 – 50). The highest value of 50.9 µm was measured for the alloy with 90% ratio of returnable material (90 – 10), which represents an increase by approximately 35% (Fig. 2c).

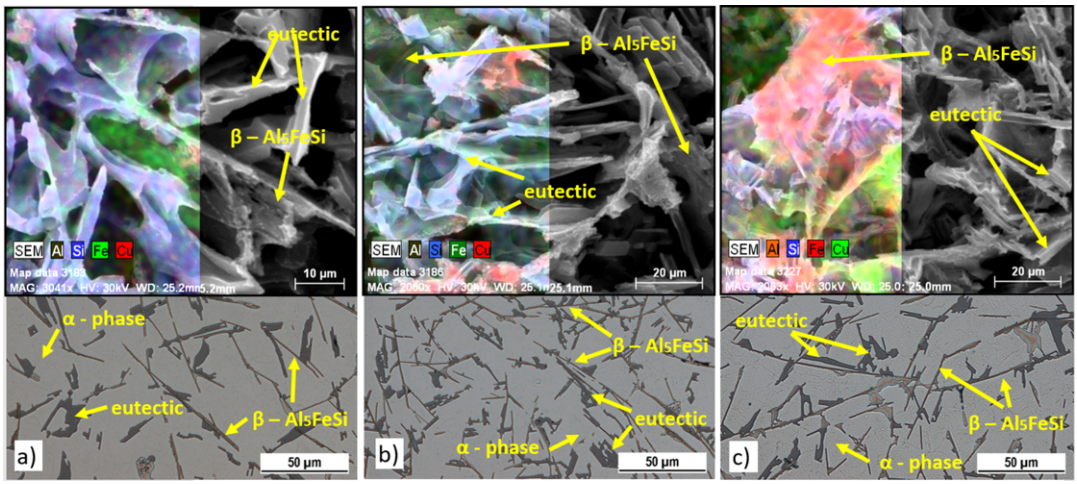

Fig. 1. Microstructure of AlSi9Cu3 alloy with different ratio of returnable material, optical microscopy, deep etch., SEM: (a) 20 – 80 alloy; (b) 50 – 50 alloy; (c) 90 – 10 alloy

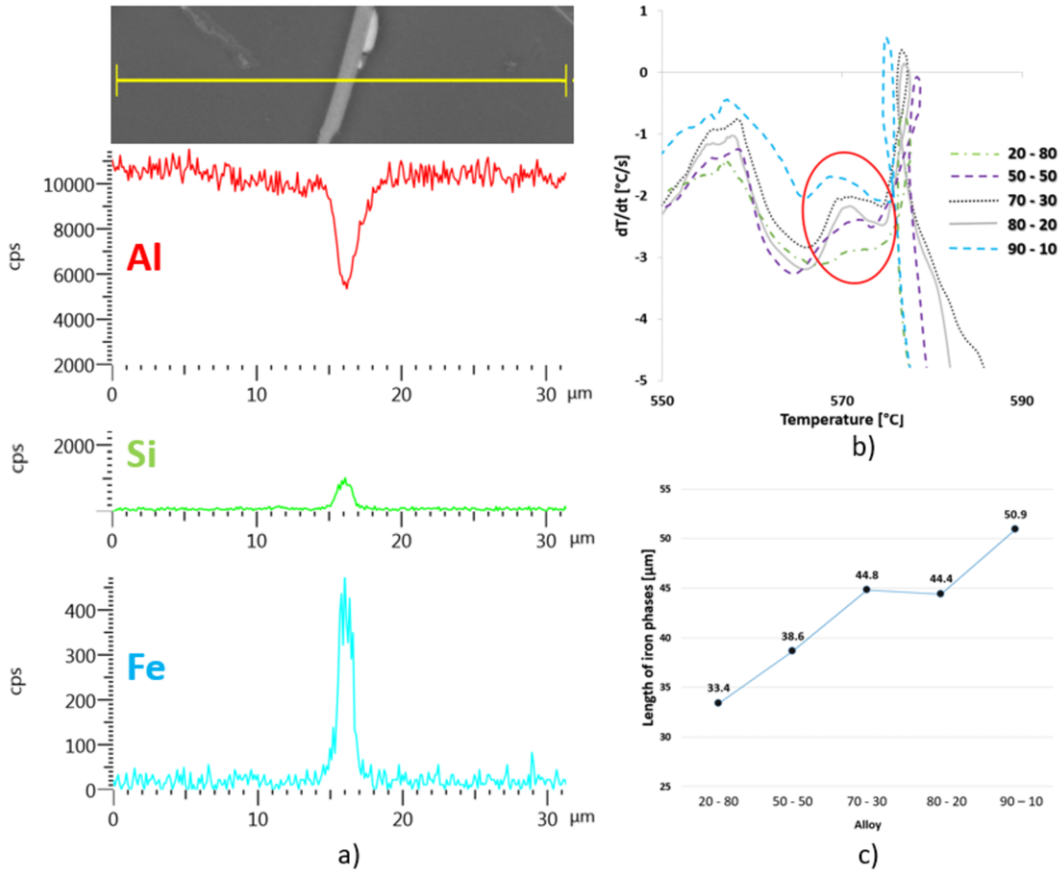

Fig. 2. (a) Line EDX analysis of 50 – 50 alloy, SEM; (b) Iron reach phases detected using first derivative curves of AlSi9Cu3 alloys in various ratio of returnable material; (c) Results of measurements of length of iron-based particles

Application of Artificially aged (T5)

There was no significant change in eutectic silicon morphology by the application of artificial aging. In the case of the 20 – 80 alloy, a hexagonal plate-like formation with a well recognizable twinning can be observed (Fig. 3a). Artificial aging caused only a local growth of the edges with arching without subsequent thinning and fragmentation. Eutectic silicon in 50 – 50, 70 – 30 and 90 – 10 alloys is, like without heat treatment, present in the non-oriented distribution of the plates, or as an unmodified eutectic, where the growth mechanism is independent of the crystallization of the α phase dendrites and thus is favorable for the formation of unbranched platelet-like formations or grains (Fig. 3b,c,d). [11].

By measuring the average lengths of the iron phase acicular formations it was found that the application of artificial aging had a positive effect on their length. The graph in Fig. 4 illustrates a reduction in the average acicular lengths of iron phase acicular formations for all alloys. It can also be seen from the graph that the efficiency of the artificial aging grew with the increasing ratio of returnable material in the batch, or with the increasing average acicular length of iron-rich phases.

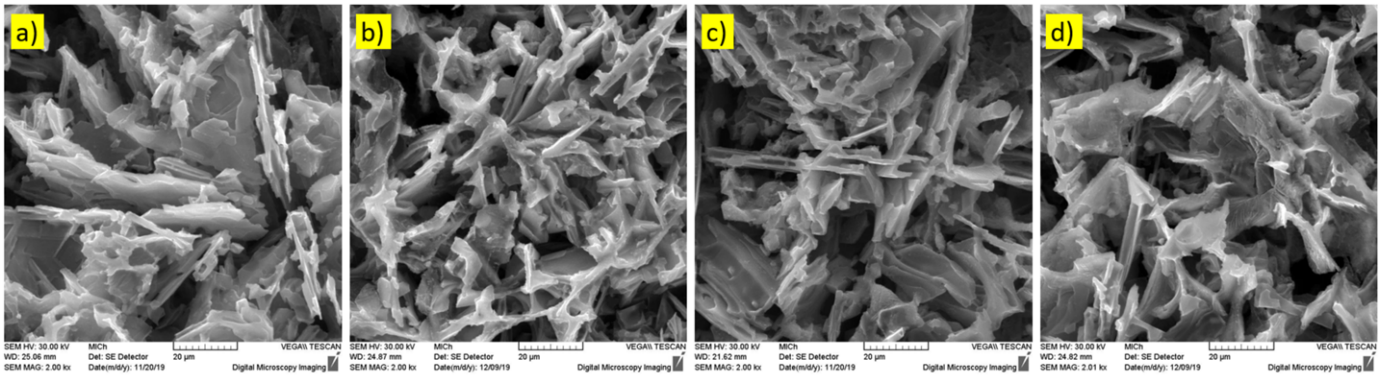

Fig. 3. Eutectic silicon after deep etching of experimental alloys after artificial ageing, SEM: (a) 20 – 80 alloy; (b) 50 – 50 alloy; (c) 70 – 30 alloy; (d) 90 – 10 alloy

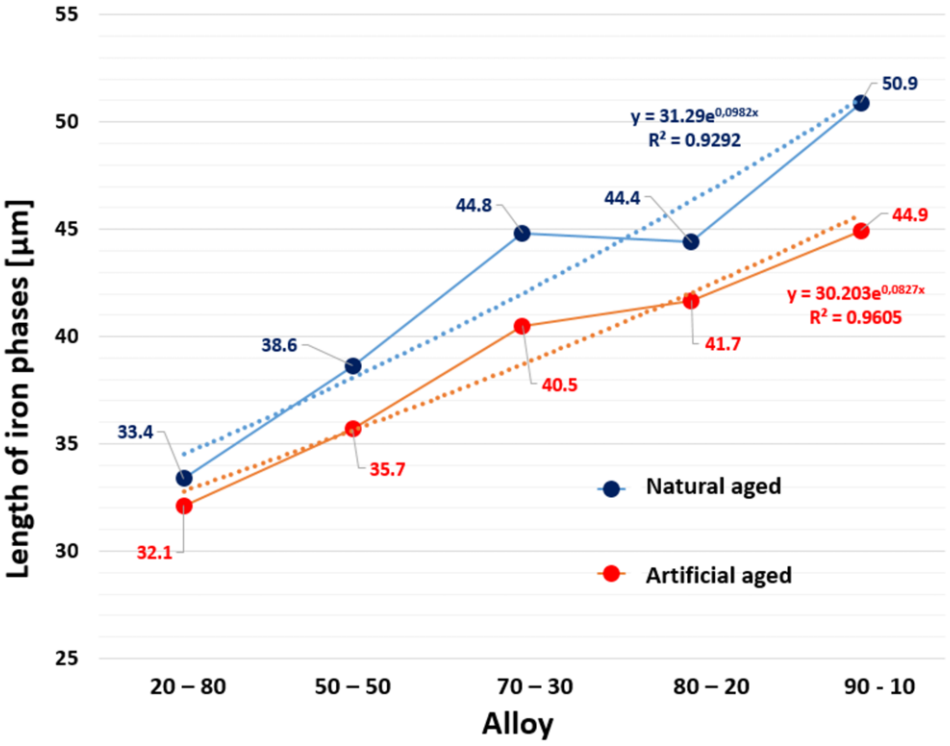

Fig. 4. Relationship between length of iron phases and alloy with various ratio of primary and returnable material and alloy state

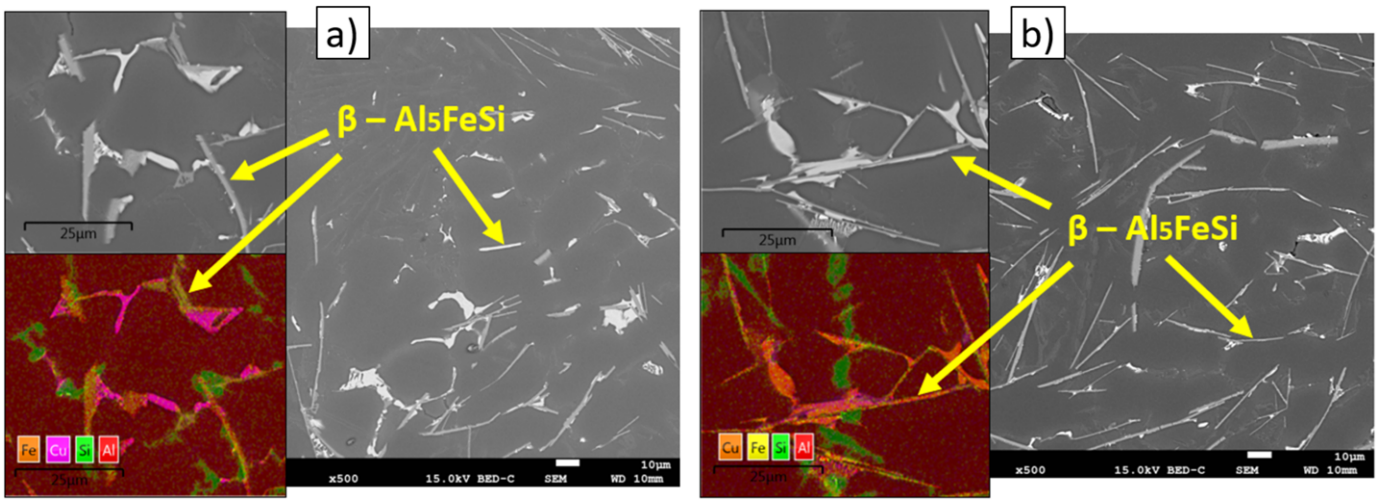

Fig. 5. Iron phases in microstructure after artificial ageing, SEM: (a) 20 – 80 alloy; (b) 90 – 10 alloy

In the 20 – 80 alloy, artificial aging resulted in a shortening of the acicular length by 1.3 µm on average compared to natural aging; in the alloy with a 90% ratio of returnable material the shortening due to artificial aging was 6 µm on average. The microstructure of 20 – 80 and 90 – 10 alloys from a scanning electron microscope and element mapping are shown in Figure 5.

We also compared the efficiency of natural and artificial aging, respectively the formation of coherence, at which the lattice deformation and internal stresses occur, thereby causing and increase in the hardness of the α-phase of the primary alloy. Based on the α-phase microhardness graph (Fig. 6) it can be concluded that artificial aging resulted in the formation of a greater number of coherent or semi-coherent precipitates in the alloy. The average values of microhardness decreased with increasing content of returnable material, while a more pronounced decrease was observed in the case of natural aging.

Mechanical properties

The results of the tensile strength tests and the agreed yield strength are shown graphically in Fig. 7. The numerical value represents the average of five measurements for both alloy conditions. As expected, best values were obtained with the alloy containing 80% primary alloy, R_m = 174 MPa, and $Rp_{0.2}$ = 97 MPa. The observed values of characteristics gradually decreased by

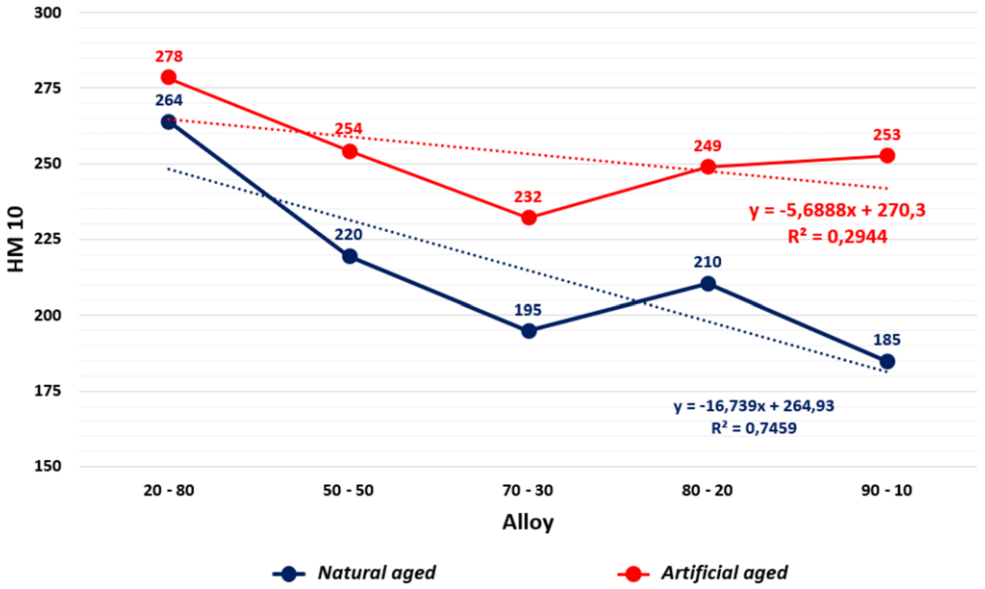

Fig. 6. Hanneman mircohardness of α-phases depending on experimental alloy and alloy state

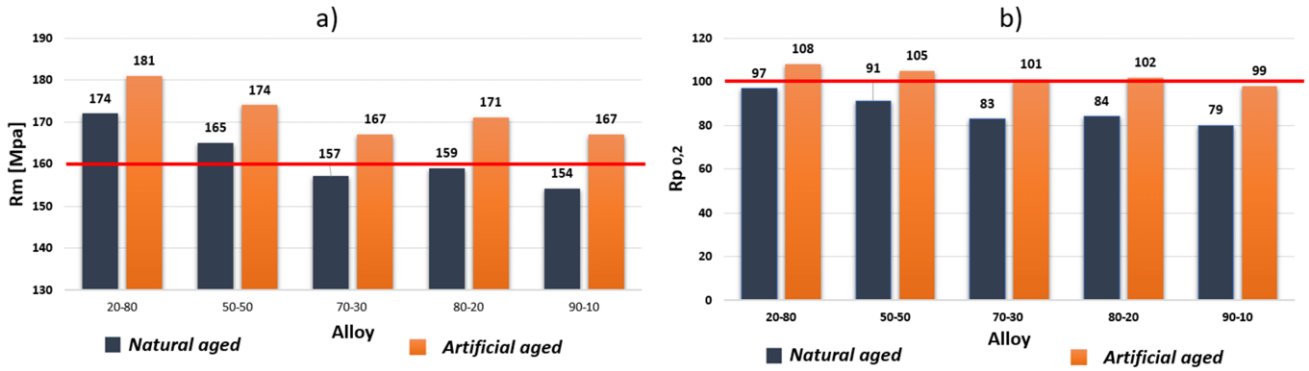

Fig. 7. (a) Tensile and (b) Yield strength depending on experimental alloy and alloy state

increasing the ratio of returnable material up to 70%. There was certain stabilization starting from the 70 – 30 alloy to the 90 – 10 alloy. The resulting values were about the same in each case. Degradation of the tensile strength and the agreed yield strength can be attributed to the increasing presence and increase in the lengths of iron phases (β – Al_5FeSi) in unfavorable acicular morphology in the structure of alloys with a higher ratio of a returnable material, thereby disrupting the structure. The shape of the iron intermetallic phase has a greater effect than its amount in the alloy. The sharp ends of the acicular phases act as stress concentrators and regions of micro-tears and tearing formation. The application of artificial aging (T5) (orange in the graph) resulted in an increase in the tensile strength and the agreed yield strength at all ratios. The red line in the graphs indicates the minimum values required by the standard (EN 17 06) for a gravity cast AlSi9Cu3 alloy in ingot molds.

A decreasing course was also observed at the evaluated ductility (Fig. 8a). Due to the increasing ratio of returnable

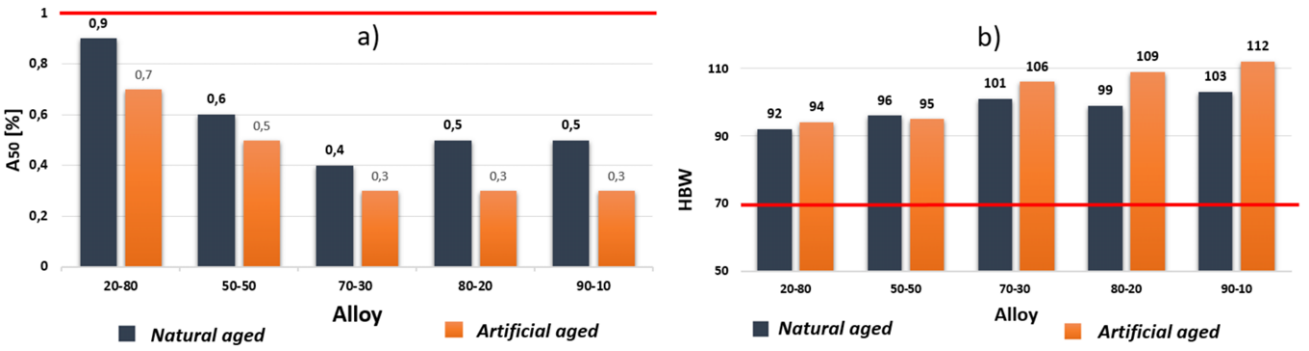

Fig. 8. (a) Ductility and (b) Brinell hardness depending on experimental alloy and alloy state

material in the batch, the ductility values dropped significantly. After artificial aging, the ductility decreased to a minimum in all cases. Hardness results (Fig. 8b) showed that as the amount of iron phases in the structure increases, the hardness values increase as well. As expected, artificial aging increased the HBW hardness values [12]. The red line in the graphs indicates the minimum values required by the standard (EN 17 06) for a gravity cast AlSi9Cu3 alloy.

Hot tearing index (HTI)

Four anchored arms of different lengths were determined for this type of quantitative tearing formation evaluation (Fig. 9a). Each one alloy was cast five times, and the cast was removed from the mold after five minutes for visual evaluation. The casting melt temperature was 750 ± 5°C, and the mold was preheated to 150 ± 10 °C. The HTI equation was used for the above-mentioned evaluation [8]. The HTI depends on the nature and size of the tears (weighting factor – WF), the number of tears (NOT) and the number of arms to be evaluated (NOF):

$$HTI = (NOT \times \sum WF) / NOF \quad (2)$$

The result of the HT index can be characterized as a measure of susceptibility to tearing formation – the so-called "Hot Tears Susceptibility" (HTS) (Table 4). The tears coefficient "WF" indicates the degree of tears severity (its characteristics and size). The WF value is divided into four categories, with each category being assigned a different numerical value. The severity of the tear and its corresponding numerical values are shown in Fig. 9b.

From the results shown in the graph (Fig. 10a) for the HT index obtained based on the equation (2) we can see that the alloy

TABLE 4

HTS intervals

HT index	< 0.5	0.5 – 1.25	1.25 – 2.25	2.25 – 3.5	> 3.5
HTS	Minimal	Low	Moderate	High	Very high

with a 20% ratio of returnable material in the batch reached an average value of 0.77 HT index, indicating low susceptibility to tears (HTS). Low susceptibility to tears (HTS) was also achieved by the balanced ratio (50 – 50) alloy with an average value of 0.99 HT index. For alloys consisting mainly of the returnable material, the resulting HT index values shifted to a moderate level of HTS tears susceptibility. The maximum HT index of 2.09 was measured in the 90 – 10 alloy, which represents an increase by approximately 3 times that of the 20 – 80 alloy. Fig. 10b clearly shows that even the 20 – 80 alloy featured sharp ends of the ferrous-phase acicular formations that acted as a critical point in the formation of micro-tears. Due to the fragility of the phase, conditions were created for further propagation of the tearing with transcrystalline characteristics. Transcrystallic tearing propagation in fragile acicular formations of ferrous phases was characteristic especially for alloys with a high ratio of returnable material, where a high occurrence of closed micro-tears in the area of fracture profile was visible (Fig. 10c).

4. Discussion

The increasing ratio of the returnable material in the AlSi9Cu3 alloy in the batch led to an increase in the Fe content and thus to the formation of harmful iron phases in all experimental alloys. The formation of a large number of iron phases in acicular morphology has already been negatively

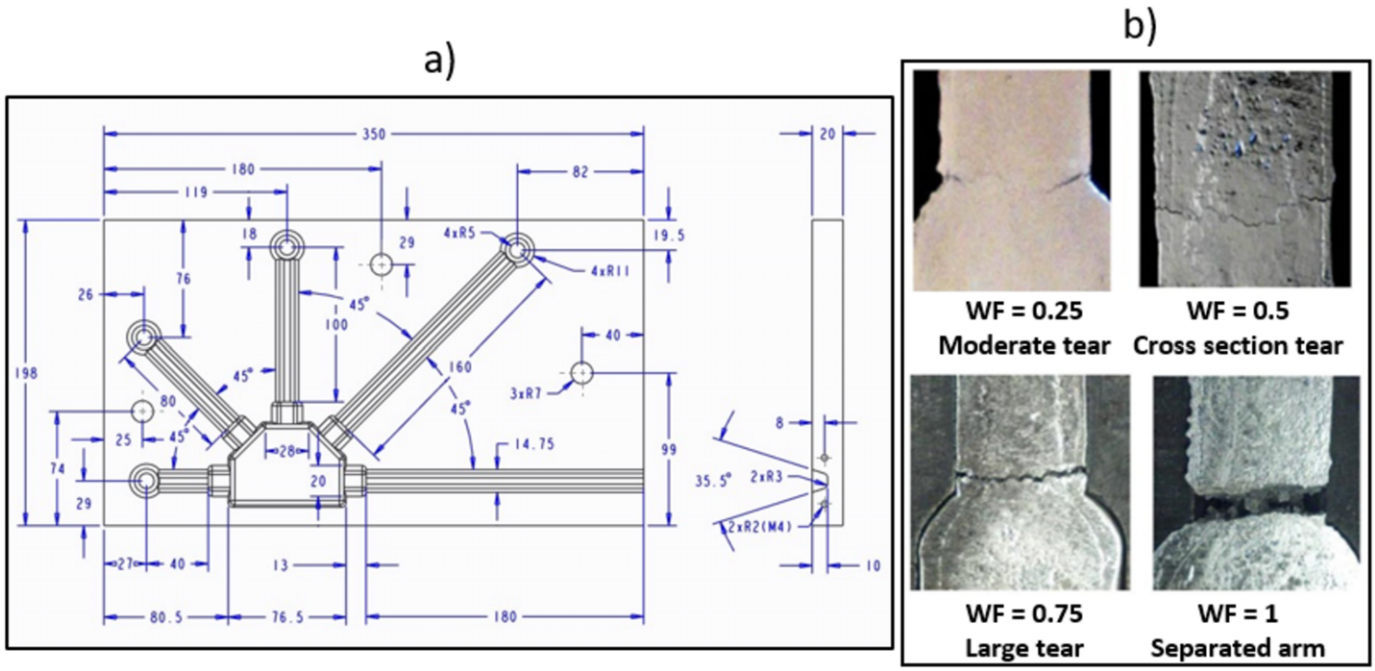

Fig. 9. Hot tearing index: (a) schematic mold; (b) weighting factor categories

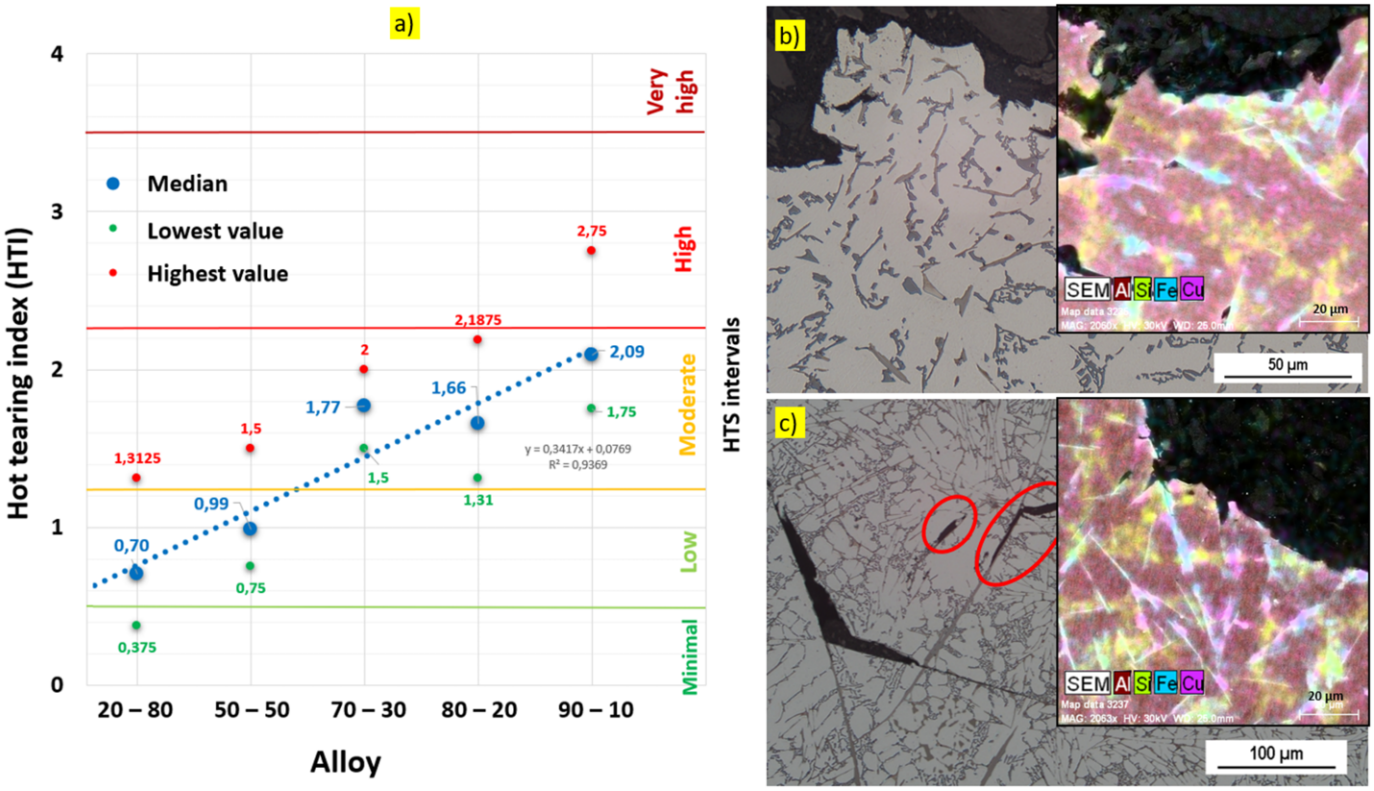

Fig. 10. AlSi9Cu3 alloy with increasing ratio of returnable material in the batch (a) Dependence of HT index; (b) Fracture profile of 20 – 80 alloy; (c) Fracture profile of 90 – 10 alloy, optical microscope, SEM – mapping

reflected in the crystallization evaluation by increasing the nucleation temperature and releasing more latent heat, which led to a gradual extension of the lengths of iron-rich phase acicular formations. Increased average lengths and increased total number of iron phases had a major effect on the degradation of the investigated mechanical characteristics except for hardness. Compared to the EN 17 06 standard, only the alloys with a high ratio of the returnable material (70 – 30, 80 – 20, 90 – 10) did not achieve the minimum required tensile strength, and none of the investigated alloys after natural aging reached the minimum agreed yield strength. Increased occurrence of iron phases was also reflected in the evaluation of the susceptibility of the alloy to tears formation. We can say that the alloy with a balanced ratio of primary alloy and returnable material (50 – 50) was just above the limit of admissibility (HTS index – slight susceptibility to tears). Newly created Al_5FeSi phase platelets were primarily formed prior to solidification of Al-Si eutectic (see Fig. 2b), which results in reducing the melt feed to critical regions in order to compensate for tears that form in the alloy and their further propagation [13]. Based on indirect methods such as density index we measured a slight increase in the amount of gas for alloys with a higher ratio of returnable material and fixation of oxide films on formed bubbles can be assumed, which may also negatively affect the mechanical properties [14].

The application of artificial aging had a positive effect on the length of the iron phase acicular formations and the local refinement of eutectic silicon, and hence on the resulting mechanical properties of the investigated alloys, which in all cases exceeded the minimum value required by the standard when assessing tensile strength and agreed yield strength. On the contrary, a negative effect of artificial aging manifested only when evaluating the ductility of alloys with different ratio of primary alloy and returnable material in the batch. Improvements in mechanical properties can also be attributed in part to the formation of coherent and semi-coherent phases formed as a result of artificial aging, the occurrence of which has been partially confirmed by measuring the microhardness of the primary α-phase. Using TEM is required to fully confirm these phases [15].

5. Conclusion

The evaluation of the obtained results confirmed the expected decrease in the overall quality of the alloy due to the increasing ratio of returnable material in the batch. It can also be concluded from the results that the gradual increase in the ratio of returnable n material has led to a visible negative effect even at balanced alloy ratios. The iron-rich phases of the alloys with a higher ratio of returnable material crystallize in the form of thicker acicular formations of considerably greater average length. The non-increasing amount of returnable material resulted in partial degradation of eutectic silicon. An important observation occurred in the case of artificial aging, which directly increased its efficiency proportionally with increasing ratio of

returnable material in the batch compared to natural aging. Alloys with a returnable material content of about 20% in the batch can also be used to produce shape-demanding castings. On the contrary, the use of alloys with a returnable material content of 50% or more for the production of shape-demanding castings in terms of tears formation can be problematic and it is rather recommended for the production of shape less-demanding and less loaded castings.

Acknowledgement

This article was created as part of the VEGA grant agency: 1/0494/17. The authors hereby thank the Agency for their support.

REFERENCES

[1] J. Gerber, Global Aluminum Recycling: A Cornerstone of Sustainable Development. International Aluminum institute, London (2009).

[2] K.S. Das, J.A.S. Gren, JOM-J. Min. Met. Mat. S. **62**, 27-31 (2010), DOI: 10.1007/s11837-010-0027-5.

[3] M.B. Djurdjevic, Z. Odanovic, N. Talijan, JOM-J. Min. Met. Mat. S. **63** (11), 51-57 (2011), DOI: 10.1007/s11837-011-0191-2.

[4] R. Podprocká, D. Bolibruchová, Archives of Foundry Engineering **17** (3), 217-221 (2017). DOI: 10.1515/afe-2017-0118.

[5] J.A. Taylor, Proc. Mat. Sci. **1**, 19-33 (2012), DOI: 10.1016/j.mspro.2012.06.004.

[6] D. Bolibruchova, L. Richtarech, S.M. Dobosz, K. Major-Gabryś, Arch. Metall. Mater. **62** (1), 339-344 (2017), DOI: 10.1515/amm-2017-0051.

[7] L. Hurtalová, T. Liptáková, E. Tillová, D. Kajánek, E. Schmidová, Metals-Basel **8** (8), 581 **(**2018), DOI: https://doi.org/10.3390/met8080581.

[8] Q. Wu, Study of Hot Tearing in Cast and Wrought Aluminum Alloys. [online] Worcester polytechnic institute, 44 (2012).

[9] D. Bolibruchová, R. Pastirčák, Foundry metallurgy of non-ferrous metals. ES ŽU Žilina, (in Slovak) (2018).

[10] M. Vončina, N. Močnik, A. Nagode, A. Stoić, M. Bizjak, The. Vjesn. **24**, 229-231 (2017), DOI: 10.17559/TV-20140922143741.

[11] C.M. Dinnis, J.A. Taylor, A.K. Dahle, Scripta Mater. **53** (8), 955-958 (2005), DOI: 10.1016/j.scriptamat.2005.06.028.

[12] M.A. Moustafa. J. Mater. Process. Tech. **1**, 209 (2009), DOI: 10.1016/j.jmatprotec.2008.02.073.

[13] J. Campbell, X. Cao, Mater. Trans. **47** (5), 1303-1312 (2006), DOI: 10.2320/matertrans.47.1303.

[14] J. Liu, Q. Wang, Y. Qi, Acta Mater. **164**, 673-682 (2019), DOI: 10.1016/j.actamat.2018.11.008.

[15] M. Vicen, P. Fabian, E. Tillová, Archives of Foundry Engineering **17** (3), 139-142 (2017), DOI: 10.1515/afe-2017-0106.